Journal of Nuclear Materials 386–388 (2009) 610–612

Contents lists available at ScienceDirect

Journal of Nuclear Materials

journal homepage: www.elsevier.com/locate/jnucmat

# Prediction of radiation-induced yield stress increment in austenitic stainless steels by using a computational approach

Chansun Shin *, Junhyun Kwon, Whungwhoe Kim

*Nuclear Materials Research Center, Korea Atomic Energy Research Institute, Daejeon 305-353, Republic of Korea*

A B S T R A C T

A computational model is presented for quantitatively estimating an increase in yield strength due to neutron irradiation by combining a cluster dynamics model and a dislocation dynamics simulation. The former calculates the concentration of point defects and defect clusters by taking into account the diffusive encounters between the point defects and the extended defects. The latter simulates the motion of dislocations in a matrix containing defect clusters. In determining the input parameters for the cluster dynamics calculations, we have obtained the primary damage parameters such as the cascade efficiency and the clustering fractions by using molecular dynamics simulations. We computed the increases in the yield strength of the austenitic stainless steels by using dislocation dynamics with the density and size distribution of radiation defects, which were obtained from the cluster dynamics calculations. The results suggest that a computational method can be a convenient tool for estimating radiation-induced hardening.



## 1. Introduction

One of the most important issues in the nuclear power industry is to assess the performance and integrity of structural materials in light water reactors. Changes in a microstructure under neutron irradiation bring about mechanical property changes of materials. Among several changes, the major concern in this study is a radiation hardening, which is generally expressed in terms of an increase in a yield strength as a function of a radiation dose. A number of reactor structural components are made of 300-series stainless steels, including the core shroud, the former, the baffle plates, etc. Accordingly, we propose a multiscale modeling approach to the theoretical estimation of a radiation hardening of austenitic stainless steels. Several computational models are involved in this study, which are molecular dynamics (MD), point defect cluster dynamics, and dislocation dynamics (DD) simulations. First, the basic radiation damage parameters are defined due to neutron irradiation to materials. The nominal displacement rates and the energy spectra of the primary knock-on atoms (PKA) are important ones, which are used as input to the following steps of the MD and the cluster dynamics calculations. In the MD simulations, we obtain the cascade related parameters such as the cascade efficiency and the fraction of a point defect clustering. And, the cluster dynamics model calculation generates the density and size of point defect clusters. Then, the changes of the yield strength are estimated from the DD calculation, which describe the interaction between the point defect clusters and the moving dislocations. The computational methods in this study present a unique way for determining the changes in the yield strength of stainless steels under neutron irradiation.

## 2. Model description and results

### 2.1. Neutron damage calculation

We applied the SPECTER code to obtain the basic neutron damage parameters – the nominal displacement rate (dpa/s) and the average PKA energy [1]. As an input to the code, the neutron spectra at the core shroud inner surface were used, which was derived from the known spectra at the reactor pressure vessel (RPV) wall in the YoungGwang 5 nuclear power plant. In estimating the neutron flux at the core shroud, we took into account the macroscopic cross section of water and stainless steels. The neutron spectra for the RPV and the core shroud are shown in Fig. 1. For the neutron spectra at the core shroud, the displacement rate is found to be $9.8 \times 10^{-8}$ dpa/s and the average PKA energy for pure iron is 5.3 keV.

### 2.2. Molecular dynamics simulation

The cascade simulations have been performed by using the MOLDY code to obtain the cascade efficiency and the clustering fractions of the point defects [2]. The simulation was continued

* Corresponding author.
*E-mail address:* cshin@kaeri.re.kr (C. Shin).

0022-3115/$ - see front matter © 2008 Elsevier B.V. All rights reserved.
doi:10.1016/j.jnucmat.2008.12.189

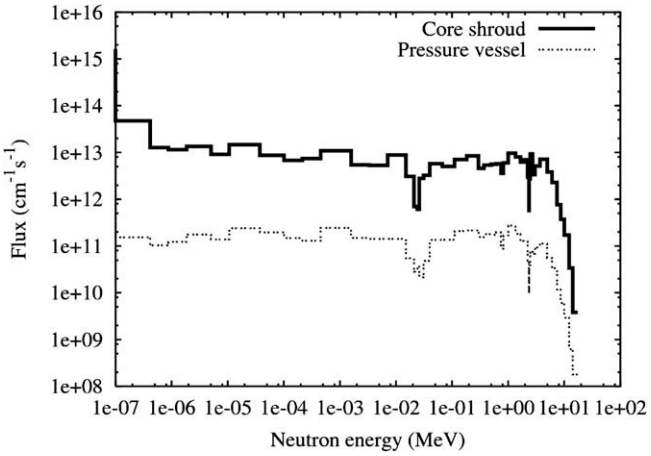


**Fig. 1.** Neutron spectra for the RPV and CS inner walls in the YoungGwang 5 nuclear power plant.

up to about 15 ps until an in-cascade recombination is complete and the atom block reaches near thermal equilibrium. The average PKA energy of 5.3 keV for iron was used to investigate the primary damage formation. This value corresponds to the MD simulation energy of 4.1 keV in that only a certain fraction of PKA energy is involved in the cascade reactions whereas the other is lost for an ionization and electronic excitation [3]. For the given energy, six simulations have been carried out with different positions and moving directions of PKA by considering a statistical variation. The cascade efficiency, defined as the ratio of the number of point defects surviving from the displacement cascade reactions to those calculated by the NRT formula [3], is found to be 0.41. The vacancy and interstitial size distributions are presented in Fig. 2. These parameters are important in that small defect clusters can provide nucleation sites for a microstructural evolution. As shown in Fig. 2, about 80% of the vacancies were isolated and those in the clusters only contained up to four vacancies. Similar results were obtained from the analysis of interstitial distribution, albeit slightly over 60% of the interstitials were observed as isolated ones.

### 2.3. Cluster dynamics model calculation

The details of the mathematical formulation for the cluster dynamics model are included in Ref. [4] and will not be repeated here. Briefly, the model describes the evolution of the point defect clusters as a consequence of cascade events, a solid state diffusion and an interaction of the point defects with sinks. This model integrates the rate equations containing the time dependency of the vacancy, interstitial concentrations and the interstitial-, vacancy-cluster ones. In solving the rate equations, it is important to determine the kinetic and material parameters of stainless steel as accurately as possible. The parameters of interest are: (1) displacement rate from the cascade reactions, (2) cascade efficiency and defect clustering fractions, (3) reaction kinetics parameters between the point defects, (4) absorption and emission rates of the point defects by and from the defect clusters, (5) annihilation kinetics for the fixed sinks for point defects such as grain boundaries, dislocations, etc. The parameters used for the cluster dynamics model calculations are listed in Table 1.

**Table 1**
Kinetic and materials parameters for stainless steels.

| Parameter | Value | Parameter | Value |
|---|---|---|---|
| Irradiation temperature (°C) | 290 | Interstitial pre-exponential factor (cm$^2$/s) | 0.066 |
| Displacement rate (dpa/s) | $9.8 \times 10^{-8}$ | Interstitial migration energy (eV) | 0.65 |
| Cascade efficiency | 0.41 | Dislocation vacancy bias | 1 |
| Interstitial clustering fraction | 0.2[a]:0.1[b]:0.03[c] | Dislocation interstitial bias | 1.25 |
| Interstitial cluster binding energy (eV) | 0.6[a]:0.85[b]:1.1[c] | Effective grain diameter (cm) | 0.0001 |
| Vacancy clustering fraction | 0.193 | Dislocation density (/cm$^2$) | $5 \times 10^{10}$ |
| Vacancy pre-exponential factor (cm/s) | 0.66 | Lattice constant of γ-iron (cm) | $3.68 \times 10^{-8}$ |
| Vacancy migration energy (eV) | 1.4 | Initial number of vacancies per cluster | 3 |

[a] Di-interstitial.
[b] Tri-interstitial.
[c] Tetra-interstitial.

The cluster dynamics calculation generates the size and density of interstitial loops as a function of a radiation dose. The evolution of these loops plays an important role in a radiation hardening through an interaction with moving dislocations. The distribution of the interstitial loops is seen in Fig. 3, where the density fraction is shown as a function of the interstitial loop size. As the dose increases, the fraction of the loops with a radius larger than 6 nm increases significantly. The total density of the interstitial loop is $1.3 \times 10^{23}$ m$^{-3}$ at 0.01 dpa, whereas the density increases to

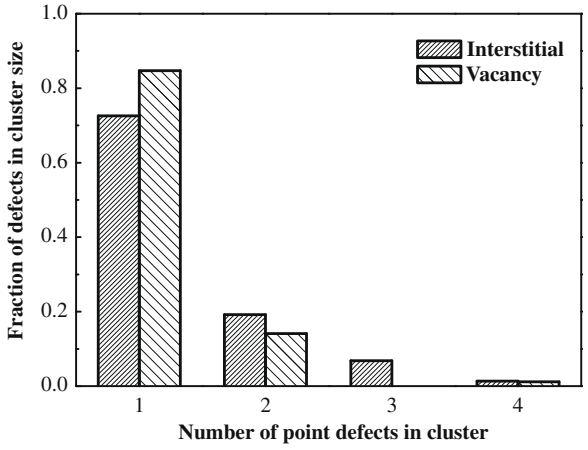


**Fig. 2.** Fractional average size distribution of defect clusters (5.3 keV-PKA at 290 °C in Fe).

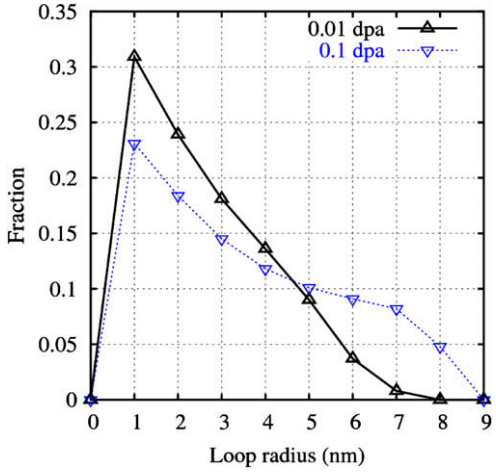


**Fig. 3.** Size distribution of the interstitial of Frank loops (total dose = 0.01 dpa).

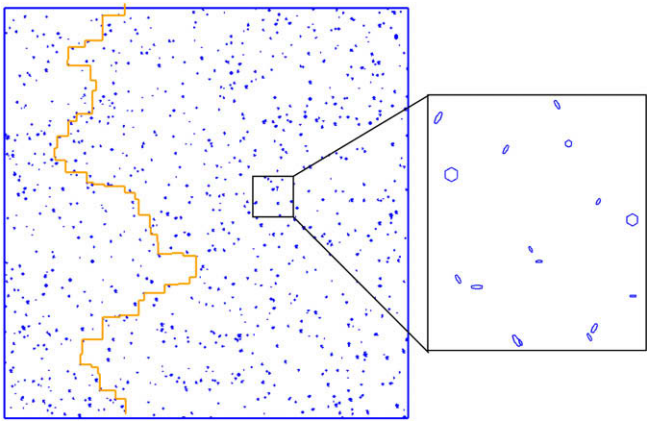

**Fig. 4.** Dislocation moving through a random array clusters.

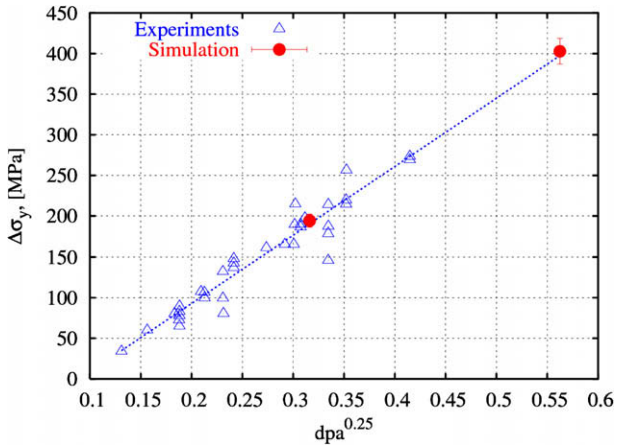


**Fig. 5.** Radiation-induced change in yield stress plotted as a function of $dpa^{0.25}$ (Triangles: Experimental data [9], Circles: Computed values from dislocation dynamics).

$2.7 \times 10^{23}$ $m^{-3}$ at 0.1 dpa. The calculated size and density of interstitial loops at 0.01 dpa correspond well with the experimental data of 316 SS specimens irradiated at 290 C and observed by using a high voltage electron microscope [5].

### 2.4. Dislocation dynamics simulations

We computed the increase in the irradiation-induced yield stress by using a discrete dislocation dynamics method [6]. The simulation volume is comprised of $X = (\bar{1}\,\bar{1}\,2)$, $Y = (1\,\bar{1}\,0)$ and $Z = (1\,1\,1)$ axis with a length of 2.87 μm, 2.83 μm and 0.69 μm, respectively. The volume represents an FCC crystal with the material properties of austenitic stainless steels used in a previous study [7]. We imposed periodic boundary conditions along the $X$ and $Y$ dimensions, which are the line and glide directions of an edge dislocation. Thus an infinitely long edge dislocation glides on a slip plane in a quasi two dimensional manner due to an applied stress. We assumed that the defects are Frank loops as observed experimentally [8]. In the simulation we represented each loop as a plane with a pre-defined barrier strength as shown in the inset of Fig. 4, and the Frank loops were randomly distributed on the four {1 1 1} habit planes. As for the barrier strength of a Frank loop, we made two assumptions: (i) the strength is proportional to a loop radius, (ii) the strength is the same for all the impact locations of a dislocation. First, we dispersed radiation-induced defects with a size distribution and density at a dose of 0.01 dpa as obtained in the previous section. Fig. 4 shows the moving edge dislocation line interacting with a Frank loop. We applied the stress incrementally while monitoring the dislocation movement, and we determined the critical shear stress $\tau_c$ at which a dislocation line moves through a random array of the Frank loops and arrives at the opposite position along the $Y$ dimension. An increase in the yield stress, $\Delta\sigma_y$ was computed by multiplying $\Delta\tau$ ($= \tau_c - \tau_m$) by the Taylor factor (~3), where $\tau_m$ is the shear stress required for the motion of a dislocation on a defect-free matrix. We adjusted the strength of a Frank loop by comparing it with the experimental data [9] for a dose level of 0.01 dpa. We obtained the best fit to the experimental data when using the strength of 13 MPa for a Frank loop with a diameter of 0.8 nm as shown in Fig. 5. The error bar of the calculated data in Fig. 5 represents the variance in $\Delta\sigma_y$ due to a change of the spatial distribution of the Frank loops. Typical values of the time step and simulation unit length used in the simulations were $10^{-10}$ s and 4 Å.

We computed an increase in the yield stress at 0.1 dpa with the found an optimum strength of a Frank loop and the size distribution and density of the Frank loops as shown in Fig. 3. It is found that the increase in the yield stress is about 402.8 MPa which corresponds well with the experimental extrapolation which is 397.3 MPa.

## 3. Discussion

We predicted radiation-induced changes in a yield stress by combining a cluster dynamics model and a dislocation dynamics method. We computed the density and the size distribution of radiation-induced defects by using the cluster dynamics model. This information was used as an input to the dislocation dynamics method. Radiation defects were distributed randomly in the simulation volume, and no clustering of the defects was considered. Defect strength was assumed to be size dependent, and took as a fitting parameter. Defect strength is, however, a complex function of interaction mechanisms between dislocations and defects [10]. Hardening due to point defects can be significant. In order to build a purely predictive model for estimating a radiation-induced hardening, we need more detailed information of defect strength such as the effects of the clustering of defects on the motion of dislocations. Atomistic simulation can be a good tool to address the detailed information of interactions between radiation defects and moving dislocations [11].

## References

[1] L.R. Greenwood, R.K. Smither, ANL/FPP/TM-197 (1985).
[2] M.W. Finnis, MOLDY – A molecular dynamics program for simulation of pure metal, Harwell Report AERE R-13182, 1988.
[3] M.J. Norgett, M.T. Robinson, I.M. Torrens, Nucl. Eng. Des. 33 (1975) 50.
[4] R.E. Stoller, Modeling the influence of irradiation temperature and displacement rate on hardening due to point defect clusters in ferritic steels, in: Effects of Radiation on Materials: 16th International Symposium, ASTM STP 1175, 1993, p. 394.
[5] N. Yoshida, H.L. Heinisch, T. Muroga, K. Araki, M. Kiritani, J. Nucl. Mater. 179–181 (1991) 1078.
[6] C.S. Shin, M.C. Fivel, M. Verdier, C. Robertson, Mater. Sci. Eng. A 400–401 (2005) 166.
[7] C. Déprés, C. Robertson, M.C. Fivel, Philos. Mag. 84 (2004) 2257.
[8] D.J. Edwards, E.P. Simonen, S.M. Bruemmer, J. Nucl. Mater. 317 (2003) 13.
[9] H.L. Heinisch, M.L. Hamilton, W.F. Sommer, P.D. Ferguson, J. Nucl. Mater. 191–194 (1992) 1177.
[10] D. Rodney, Nucl. Instrum. and Meth. B. 228 (2005) 100.
[11] Y.N. Osetsky, D. Rodney, D.J. Bacon, Philos. Mag. 86 (2006) 2295.